INTERNATIONAL JOURNAL OF PRECISION ENGINEERING AND MANUFACTURING Vol. 16, No. 2, pp. 323-333 FEBRUARY 2015 / 323
DOI: 10.1007/s12541-015-0043-z

Delamination Buckling of a Thin Film Bonded to an Orthotropic Substrate

Xiao Ru Zhuo[1], Hyun Seok Jang[1], and Hyeon Gyu Beom[1,#]

1 Department of Mechanical Engineering, College of Engineering, Inha University, 100, Inha-ro, Nam-gu, Incheon, 402-751, South Korea
Corresponding Author / E-mail: hgbeom@inha.ac.kr, TEL: +82-32-860-7310, FAX: +82-32-868-1716

KEYWORDS: Buckling delamination, Film/substrate structure, Orthotropic material, Energy release rate, Mode mixity

This paper investigates the delamination buckling of an orthotropic film with compressive prestress bonded to an orthotropic substrate. The buckled film detached from the film/substrate structure is solved in the closed form except for the resultant force and bending moment at the ends of the buckled film, which are obtained by matching the solutions for the buckled film and the film/substrate structure in which the buckled part of the film is removed. Special attention is paid to the effects of parameters of orthotropic materials on delamination buckling based on a numerical analysis. The energy release rate and mode mixity induced by buckling are evaluated, and the growth and arrest of the interface crack under mixed loading induced by buckling are discussed based on the energy criterion.

Manuscript received: March 9, 2014 / Revised: October 19, 2014 / Accepted: November 10, 2014

NOMENCLATURE

a_{ij} = dimensionless compliance coefficient
$\mathbf{B}$ = complex matrix
b = half debonding size
D = bending stiffness
G = energy release rate
$g_i(z)$ = complex function
$\mathbf{H}$ = complex matrix
h = thickness of a film
$\mathbf{I}$ = identity matrix
K_i^*, $\mathbf{k}$ = stress intensity factor
M, M_0 = bending moment
N, N_0 = resultant force
p, p_i = complex number
S_{ij}, S^e_{ij} = conventional compliance component
u_i, u^N, u^M = displacement
$\mathbf{Y}(\zeta_1, \zeta_2)$ = matrix function
$\boldsymbol{\alpha}$ = bimaterial matrix
α_0 = bimaterial parameter
$\boldsymbol{\beta}$ = bimaterial matrix
β_0 = bimaterial parameter
Γ = interface fracture toughness
ΔN = change in resultant force
ε_{ij} = strain component
ζ = dimensionless resultant force
θ_0 = rotation angle
κ_{ij} = thermal expansion coefficient
λ, λ_i = orthotropic parameter
ρ, ρ_i = orthotropic parameter
σ = stress
$\phi(x_1, x_2)$ = complex function vector
χ = dimensionless bending moment
ψ = mode mixity

1. Introduction

Layered structures composed of a thin film and a substrate have found wide technical applications in electronic devices, semiconductors, and optical electronics. An interface crack between a thin film and a substrate does not disturb elastic fields in the bimaterial structure under uniform thermal loading or applied loads, and stress intensity factors at the crack tip are not induced. The buckling of a film with compressive prestress induced by a temperature change or applied load can redistribute displacements and stresses in the bimaterial structure. Stress intensity factors are induced by buckling, and film buckling can drive interface decohesion as a result of crack growth. Therefore, delamination buckling can reduce the reliability of the bimaterial structure. The last several decades have witnessed an increasing number of studies paying close attention to buckling problems. Whitcomb[1] examined the buckling of a delaminated region in a laminated composite subjected to compressive loads by calculating critical loads for delamination growth based on criteria for the energy release rate. Hutchinson and Suo[2] considered the delamination of a thin film as a result of buckling and discussed the extent of interface decohesion driven by buckling. Choi et al.[3] investigated edge and buckling delamination in multilayer thermal barrier coatings and showed that large scale delamination can arise when the top coat is stiff. Bruno and Greco[4] analyzed delamination buckling and growth in layered plates with finite thickness and proposed a general model of these plates to examine the global instability of the whole plate in conjunction with the local instability of layers. Cotterell and Chen[5] and Yu and Hutchinson[6] investigated the effects of material parameters on the buckling delamination of thin films on the isotropic substrate and solved the problem of the buckled film by using a matching technique. Jeong and Beom[7] provided a buckling analysis of an orthotropic layer bonded to a substrate with an interface crack under a compressive load and obtained critical loads at the onset of buckling by using the Fourier transform method. Recently, Lu et al.[8] examined the buckling delamination of ultra thin films based on the theory of elastic material surfaces.[9] In general, previous studies have focused on delamination buckling in isotropic layered structures. That is, few have paid close attention to the effects of parameters of orthotropic materials on the bucking delamination of thin films.

The purpose of this paper is to investigate the delamination buckling of a film bonded to an orthotropic substrate with an interface crack. The buckling of a film with compressive prestress redistributes displacements and stresses in the bimaterial structure. The buckled part of the film with prestress and the remaining part of the film/substrate structure are considered separately, and the film detached from the film/substrate structure is solved based on von Karman nonlinear plate theory. The film/substrate structure in which the buckled part of film is removed is treated as a linear plane strain problem and solved numerically by using the finite element method. The complete solution is then determined from matching solutions for the buckled film and the film/substrate structure in which the buckled part of the film is removed. Special attention is paid to the effects of parameters of orthotropic materials on delamination buckling. The energy release rate and mode mixity for the interface crack as a result of buckling are evaluated using solutions for the resultant force and bending moment at the edge of the buckled film. In addition, the growth and arrest of the interface crack under mixed loading induced by buckling are considered based on the energy criterion.

2. Buckling of a Thin Film Bonded to an Orthotropic Substrate

Consider a film bonded to an orthotropic substrate with the initial debonding of size $2b$, as shown in Fig. 1(a). The thickness of the film is h, and the substrate is a half plane of infinite extent. Cartesian coordinates x_1, x_2, and x_3 are chosen to coincide with the principle axes of the orthotropic material. Initially, the film/substrate structure is free of any stress, which is referred to as a stress-free state. If the temperature of the film/substrate structure changes by ΔT from the stress-free state, then stresses can be induced in the film because of a thermal expansion mismatch between the film and the substrate. The induced stress in the film can be expressed as follows:[10]

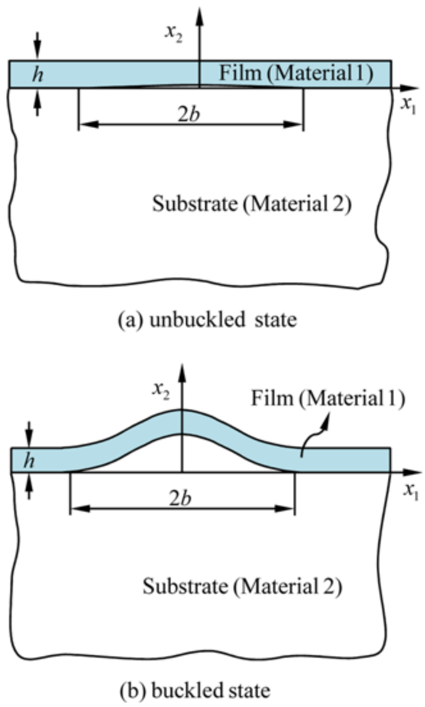

Fig. 1 Geometry of a film/substrate structure with an interface crack under a temperature change

$$\sigma_{11} = -\sigma \tag{1}$$

where

$$\sigma = \frac{1}{S_{11}^{(1)}S_{33}^{(1)} - S_{13}^{(1)2}}[S_{33}^{(1)}(\kappa_{11}^{(1)} - \kappa_{11}^{(2)}) - S_{13}^{(1)}(\kappa_{33}^{(1)} - \kappa_{33}^{(2)})]\Delta T \tag{2}$$

where S_{ij} are the conventional compliance components and κ_{11} and κ_{33} are the thermal expansion coefficients in the directions of x_1 and x_3 axes, respectively. Here the superscripts 1 and 2 in parentheses indicate the quantities taken for the film (material 1) and the substrate (material 2), respectively, which holds for the whole paper. The film/substrate structure with the initial delamination and residual compression is susceptible to buckling. If the initial delamination and compressive stress satisfy a critical condition, then the film undergoes thermally induced buckling, as shown in Fig. 1(b).

Now consider a film/substrate structure with the same geometric configuration as the one described earlier (see Fig. 2). The structure is subject to externally applied uniform strain $\varepsilon_{11} = -\varepsilon^{\infty}$, which leads to uniformly distributed compressive stress σ in the film. Under the plane strain condition, σ is given by

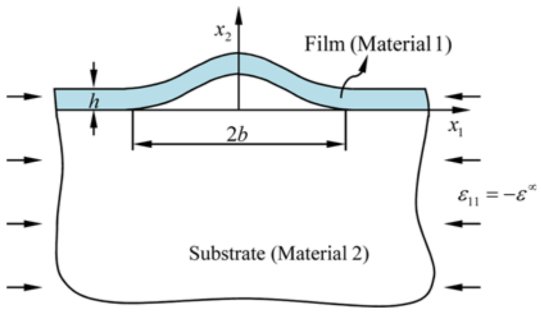

Fig. 2 Delamination buckling of a film/substrate structure under applied compressive strain

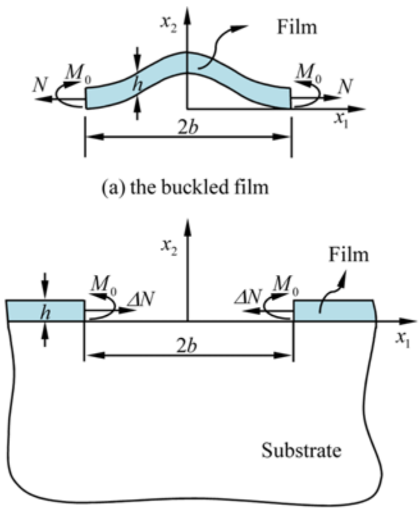

(a) the buckled film

(b) the film/substrate structure in which the buckled part of film is removed

Fig. 3 A film/substrate structure with buckling delamination

$$\sigma=\frac{\varepsilon^{\infty}}{S_{11}^{e(1)}} \tag{3}$$

where

$$S_{11}^{e}=S_{11}-\frac{S_{13}^{2}}{S_{33}} \tag{4}$$

and the superscript e indicates the quantity for the plane strain problem. In the unbuckled state, the stress field in the film is uniform, and stress intensity factors at crack tips vanish. When buckling occurs in the film, however, stress intensity factors are induced. Therefore, film buckling can drive the extent of interface decohesion.

Buckling induced by a temperature change or applied load causes the redistribution of displacements and stresses in the bimaterial structure. Here the disturbance of elastic fields measured from the unbuckled state with prestress $\sigma_{11}=-\sigma$ is examined. The problem of the buckled film bonded to a substrate can be solved by using the matching technique.[5] The buckled part of the film with prestress $\sigma_{11}=-\sigma$ and the remaining film/substrate structure, as shown in Fig. 3, are solved separately. Then a complete solution is determined by matching solutions for the buckled film and the remaining film/substrate structure at the edges of the film.

3. Nonlinear Solution for the Buckled Film

According to Hutchinson and Suo,[2] a film detached from the film/substrate structure, as shown in Fig. 3(a), can be formulated based on von Karman nonlinear plate theory.[11] The resultant force for the buckled state can be expressed as

$$N=\Delta N-\sigma h \tag{5}$$

where N is the resultant force per unit length and ΔN is the change in the resultant force induced by buckling. Here ΔN is related to strain ε_{11} by

$$\Delta N=\frac{h}{S_{11}^{e(1)}}\varepsilon_{11} \tag{6}$$

$$\varepsilon_{11}=u_{1,1}+\frac{1}{2}(u_{2,1})^{2} \tag{7}$$

where u_1 and u_2 are displacements in the buckled film and comma (,) denotes a partial derivative with respect to Cartesian coordinates. Here u_1 and u_2 are measured from the unbuckled state with prestress $\sigma_{11}=-\sigma$, which is chosen as the reference configuration. The bending moment in the buckled film is expressed as

$$M=Du_{2,11} \tag{8}$$

where M is the bending moment per unit length and D is bending stiffness given by

$$D=\frac{1}{12}\frac{h^{3}}{S_{11}^{e(1)}} \tag{9}$$

Equilibrium equations for the buckled film require

$$\Delta N_{,1}=0\,,\;\; Du_{2,1111}-Nu_{2,11}=0 \tag{10}$$

Note that ΔN is a constant in the buckled film from Eq. (10). Therefore, N can be taken as $N=-N_0$ where N_0 is a compressive resultant force at the end of the buckled film. By solving Eq. (10) with Eqs. (6) and (7), displacements u_1 and u_2 can be obtained as

$$\begin{aligned} u_1(x_1)&=S_{11}^{e(1)}(-N_0+\sigma h)\frac{x_1}{h}-\frac{1}{8}\frac{M_0^{2}}{D^{2}\xi^{3}\cos^{2}\xi b}(2\xi x_1-\sin 2\xi x_1)\\ u_2(x_1)&=\frac{M_0}{D\xi^{2}\cos\xi b}(\cos\xi b-\cos\xi x_1) \end{aligned} \tag{11}$$

where

$$\xi^{2}=\frac{N_0}{D}\,,\;\; M_0=M(\pm b) \tag{12}$$

In obtaining Eq. (11), the following symmetry conditions were used for the buckled film:

$$u_1(0)=0\,,\;\; u_2(\pm b)=0\,,\;\; u_{2,1}(0)=u_{2,111}(0)=0 \tag{13}$$

The displacement and rotation at the edge of the buckled film are obtained from Eq. (11) as

$$\begin{aligned} u_0&=-S_{11}^{e(1)}(-N_0+\sigma h)\frac{b}{h}+\frac{1}{8}\frac{M_0^{2}}{D^{2}\xi^{3}\cos^{2}\xi b}(2\xi b-\sin 2\xi b)\\ \theta_0&=\frac{M_0\xi}{N}\tan\xi b \end{aligned} \tag{14}$$

where

$$u_0 = u_1(-b) = -u_1(b)\,,\;\; \theta_0 = u_{2,1}(-b) = -u_{2,1}(b) \tag{15}$$

The undetermined N_0 and M_0 in Eq. (11) are found by performing the matching of u_0 and θ_0 at the ends of the buckled film. In particular, solutions to N_0 and M_0 for the film clamped on its edges (u_0=θ_0=0) can be expressed in the dimensionless form as

$$\zeta = 1\,,\;\; \chi = \frac{1}{\sqrt{3}}\sqrt{\frac{\sigma}{\sigma_c} - 1} \tag{16}$$

where

$$\zeta = \frac{N_0}{h\sigma_c}\,,\;\; \chi = \frac{M_0}{h^2\sigma_c} \tag{17}$$

$$\sigma_c = \frac{\pi^2}{12}\frac{1}{S_{11}^{e(1)}}\left(\frac{h}{b}\right)^2 \tag{18}$$

Here ζ and χ are the dimensionless resultant force and bending moment, respectively. When $\sigma = \sigma_c$, $u_2(x_1)$=0, whereas $u_2(x_1)\neq 0$ for $\sigma > \sigma_c$. Therefore, σ_c is the critical stress at the onset of buckling for a film clamped on its edges. Hutchinson and Suo[2] also derived Eq. (17) for isotropic cases.

4. Plane Strain Problem for A Film/Substrate System

Consider a film/substrate structure in which the buckled part of the film is removed, as shown in Fig. 3(b). Here the focus is on the disturbance of elastic fields from the buckling of the film. The resultant force ΔN and the bending moment M_0 are applied at the boundaries x_1=±b and 0<x_2<h. The film/substrate structure can be treated as the linear problem of plane strain.[5,6] According to Cotterell and Chen,[5] the displacement u_0 and the rotation angle θ_0 at x_1=–b for the buckled film can be expressed as

$$\begin{aligned} u_0 &= a_{11}\frac{bS_{11}^{e(1)}}{h}\Delta N - a_{12}\frac{bS_{11}^{e(1)}}{h^2}M_0 \\ \theta_0 &= -a_{21}\frac{bS_{11}^{e(1)}}{h^2}\Delta N + a_{22}\frac{bS_{11}^{e(1)}}{h^3}M_0 \end{aligned} \tag{19}$$

where a_{ij} $(i, j = 1, 2)$ is the dimensionless symmetric compliance coefficient. With the strain energy expression for the film/substrate structure without the buckled part of the film,

$$\Delta N u_0 + M_0\theta_0 = \int_0^h \sigma_{11}(-b,x_2)u_1(-b,x_2)dx_2 \tag{20}$$

where

$$\sigma_{11}(-b,x_2) = \frac{\Delta N}{h} - \frac{12M_0}{h^3}\left(x_2 - \frac{h}{2}\right) \tag{21}$$

the displacement $u_1(-b, x_2)$ for the problem of plane strain can be written as

$$u_1(-b,x_2) = \Delta N\frac{bS_{11}^{e(1)}}{h}u^N - M_0\frac{bS_{11}^{e(1)}}{h^2}u^M \tag{22}$$

Here the dimensionless displacements u^N and u^M are (see Appendix A)

$$\begin{aligned} u^N &= u^N\left(\frac{x_2}{h}, \frac{b}{h}, \alpha_0, \beta_0, \gamma_0, \rho_1, \lambda_1\right) \\ u^M &= u^M\left(\frac{x_2}{h}, \frac{b}{h}, \alpha_0, \beta_0, \gamma_0, \rho_1, \lambda_1\right) \end{aligned} \tag{23}$$

where

$$\lambda = \frac{S_{11}^e}{S_{22}^e}\,,\;\; \rho = \frac{2S_{12}^e + S_{66}^e}{2\sqrt{S_{11}^e S_{22}^e}} \tag{24}$$

$$\alpha_0 = \frac{(nS_{11}^e)^{(2)} - (nS_{11}^e)^{(1)}}{(nS_{11}^e)^{(2)} + (nS_{11}^e)^{(1)}}$$

$$\beta_0 = \frac{(\sqrt{S_{11}^e S_{22}^e} + S_{12}^e)^{(2)} - (\sqrt{S_{11}^e S_{22}^e} + S_{12}^e)^{(1)}}{2\left[\left\{\left(\lambda^{-\frac{1}{4}}nS_{11}^e\right)^{(2)} + \left(\lambda^{-\frac{1}{4}}nS_{11}^e\right)^{(1)}\right\}\left\{\left(\lambda^{-\frac{3}{4}}nS_{11}^e\right)^{(2)} + \left(\lambda^{-\frac{3}{4}}nS_{11}^e\right)^{(1)}\right\}\right]^{\frac{1}{2}}} \tag{25}$$

$$\gamma_0 = \frac{\lambda_2}{\lambda_1}$$

$$S_{ij}^e = S_{ij} - \frac{S_{i3}S_{j3}}{S_{33}} \tag{26}$$

$$n = \sqrt{\frac{1}{2}(\rho + 1)} \tag{27}$$

Subscripts 1 and 2 added to λ and ρ indicate materials 1 and 2, respectively. Here, λ and ρ are orthotropic parameters which measure the degree of orthotropy of materials. α_0, β_0, and γ_0 are bimaterial parameters which measure the elastic mismatch between two materials. These three bimaterial constants can be regarded as the generalized Dundurs parameters for the orthotropic bimaterial. The material parameters needed to describe u^N and u^M are determined using the modified Stroh formalism.[10,12] Eqs. (19), (20), (21), and (22) provide

$$a_{11} = \int_0^1 u^N d\left(\frac{x_2}{h}\right),\;\; a_{12} = a_{21} = \frac{1}{2}\int_0^1\left[u^M + 12\left(\frac{x_2}{h} - \frac{1}{2}\right)u^N\right]d\left(\frac{x_2}{h}\right),$$

$$a_{22} = 12\int_0^1\left(\frac{x_2}{h} - \frac{1}{2}\right)u^M d\left(\frac{x_2}{h}\right) \tag{28}$$

It is clear from Eqs. (23) and (28) that

$$a_{ij} = a_{ij}\left(\frac{b}{h}, \alpha_0, \beta_0, \gamma_0, \rho_1, \lambda_1\right) \tag{29}$$

The orthotropic rescaling method[10] provides the explicit dependence of a_{ij} on λ_1. By applying this method to the problem of plane strain, it can be shown that (see Appendix B)

$$a_{ij} = a_{ij}\left(\frac{b}{h}, \alpha_0, \beta_0, \gamma_0, \rho_1, \lambda_1\right) = \hat{a}_{ij}\left(\lambda_1^{\frac{1}{4}}\frac{b}{h}, \alpha_0, \beta_0, \gamma_0, \rho_1\right) \tag{30}$$

where

$$\hat{a}_{ij}\left(\lambda_1^{\frac{1}{4}}\frac{b}{h}, \alpha_0, \beta_0, \gamma_0, \rho_1\right) = a_{ij}\left(\lambda_1^{\frac{1}{4}}\frac{b}{h}, \alpha_0, \beta_0, \gamma_0, \rho_1, 1\right) \tag{31}$$

Note that a_{ij} depends only on five parameters ($\lambda_1^{\frac{1}{4}}\, b/h$, α_0, β_0, γ_0, and ρ_1).

Once the dimensionless displacements u^N and u_M are determined, the compliance coefficients a_{ij} $(i, j = 1, 2)$ can be evaluated from Eq. (28).

To obtain u^N and u^M, finite element analyses are conducted using the commercial program ABAQUS. Based on the results of u^N and u^M obtained from finite element analyses, a_{ij} $(i, j = 1, 2)$ are calculated. Particularly, the numerical results for a_{11}, a_{12}, and a_{22} for the cases α_0=0 and α_0=0.9 are consistent with previous results given by Yu and Hutchinson.[6]

5. Resultant Force and the Bending Moment

The undetermined dimensionless resultant force ζ and the bending moment χ can be obtained by performing the matching of u_0 and θ_0 at the ends of the buckled film. Matching Eqs. (14) and (19) produces

$$(1+a_{11})\left(\frac{\sigma}{\sigma_c}-\zeta\right)-\frac{3}{2\pi}\sqrt{\zeta}\left(\frac{\chi}{\zeta\cos\sqrt{\zeta}}\right)^2(2\pi\sqrt{\zeta}-\sin 2\pi\sqrt{\zeta})-a_{12}\chi = 0$$

$$\frac{\chi}{\sqrt{\zeta}}\tan\pi\sqrt{\zeta}+\frac{\pi}{12}a_{22}\chi-\frac{\pi}{12}a_{21}\left(\frac{\sigma}{\sigma_c}-\zeta\right) = 0 \tag{32}$$

It is apparent from Eq. (32) that

$$\zeta = \zeta\left(\frac{\sigma}{\sigma_c}, a_{ij}\right),\quad \chi = \chi\left(\frac{\sigma}{\sigma_c}, a_{ij}\right) \tag{33}$$

From Eqs. (30) and (33), it can be shown that

$$\zeta = \zeta\left(\frac{\sigma}{\sigma_c}, \lambda_1^{\frac{1}{4}}\frac{b}{h}, \alpha_0, \beta_0, \gamma_0, \rho_1\right)$$
$$\chi = \chi\left(\frac{\sigma}{\sigma_c}, \lambda_1^{\frac{1}{4}}\frac{b}{h}, \alpha_0, \beta_0, \gamma_0, \rho_1\right) \tag{34}$$

By using the relationship

$$\lambda_1^{\frac{1}{4}}\frac{b}{h} = \frac{\pi}{2\sqrt{3}}\frac{1}{[\sqrt{S_{11}^{e(1)}S_{22}^{e(1)}}\sigma]^{\frac{1}{2}}}\sqrt{\frac{\sigma}{\sigma_c}} \tag{35}$$

Eq. (34) can be rewritten as

$$\zeta = \zeta(\sqrt{\sigma/\sigma_c}, \sqrt{S_{11}^{e(1)}S_{22}^{e(1)}}\sigma, \alpha_0, \beta_0, \gamma_0, \rho_1)$$
$$\chi = \chi(\sqrt{\sigma/\sigma_c}, \sqrt{S_{11}^{e(1)}S_{22}^{e(1)}}\sigma, \alpha_0, \beta_0, \gamma_0, \rho_1) \tag{36}$$

Note that ζ and χ are functions of six parameters ($\sqrt{\sigma/\sigma_c}$, $\sqrt{S_{11}^{e(1)}S_{22}^{e(1)}}\sigma$, α_0, β_0, γ_0, and ρ_1).

Since the numerical results for a_{ij} have been obtained, ζ and χ can be calculated by solving Eq. (32) numerically once $\sqrt{S_{11}^{e(1)}S_{22}^{e(1)}}\sigma$ is given. The prestress $\sqrt{S_{11}^{e(1)}S_{22}^{e(1)}}\sigma$ is taken to be 10^{-3} in all calculations.

6. Energy Release Rate and Mode Mixity

The buckling of a thin film bonded to an orthotropic substrate induces nonzero interface stress intensity factors. The energy release rate and mode mixity of the interface crack in a bimaterial structure with a buckled film can be approximately evaluated for most relevant values of b/h by using solutions to the problem of a semi-infinite interface crack in a bimaterial structure consisting of an orthotropic film/substrate, as shown in Fig. 4.[2,6] The energy release rate is the energy released during the creation of per unit area of new crack area. In the problem of a semi-infinite crack, the resultant force ΔN and the bending moment M_0 per unit length are applied to the film at x_1=–∞. The energy release rate of the interface crack, denoted by G, is given as follows:[10,13]

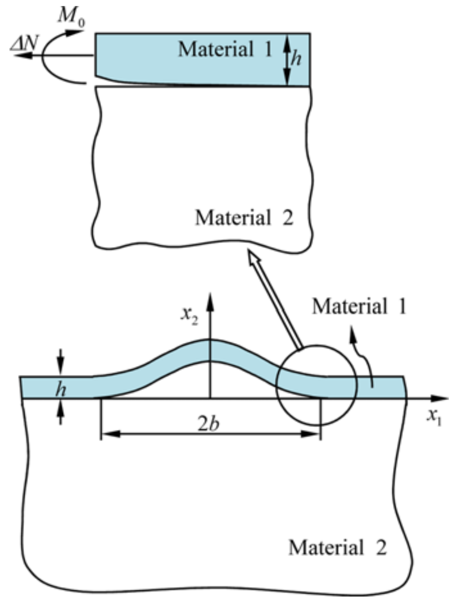

Fig. 4 Edge delamination model of a film/substrate structure near the crack tip

$$G = \frac{1}{2}S_{11}^{e(1)}\left[\frac{12M_0^2}{h^3}+\frac{(\Delta N)^2}{h}\right] \tag{37}$$

By using Eq. (17), Eq. (37) can be rewritten in the following dimensionless form:

$$G^* = \frac{G}{G_0} = 12\left(\frac{\sigma_c}{\sigma}\chi\right)^2+\left(1-\zeta\frac{\sigma_c}{\sigma}\right)^2 \tag{38}$$

where G^* is the normalized energy release rate and G_0, defined as

$$G_0 = \frac{1}{2}S_{11}^{e(1)}h\sigma^2 \tag{39}$$

is the strain energy per unit area stored in the unbuckled film available for dissipation. From Eqs. (36) and (38), it is easily seen that G^* depends on six parameters ($\sqrt{\sigma/\sigma_c}$, $\sqrt{S_{11}^{e(1)}S_{22}^{e(1)}}\sigma$, α_0, β_0, γ_0, and ρ_1). For the case of the film clamped on its edges with the solutions for ζ and χ in Eq. (16), Eq. (38) reduces to

$$\frac{G}{G_0} = \left(1-\frac{\sigma_c}{\sigma}\right)\left(1+3\frac{\sigma_c}{\sigma}\right) \tag{40}$$

Because the dimensionless functions ζ and χ for various combinations of the six parameters are determined, G^* can be numerically calculated using Eq. (38). The numerical results of G^* are plotted as a function of $\sqrt{\sigma/\sigma_c}$ for various combinations of material parameters in Fig. 5. Here $\sqrt{S_{11}^{e(1)}S_{22}^{e(1)}}\sigma=10^{-3}$ is used. For isotropic bimaterial cases, the numerical results are generally consistent with those in Yu and Hutchinson.[6] Regardless of the material parameters (α_0, β_0, γ_0, and ρ_1), G^* increases rapidly as $\sqrt{\sigma/\sigma_c}$ increases, peaking at $1 < \sqrt{\sigma/\sigma_c} < 2$. Then it is followed by a decreasing trend and eventually converges to the

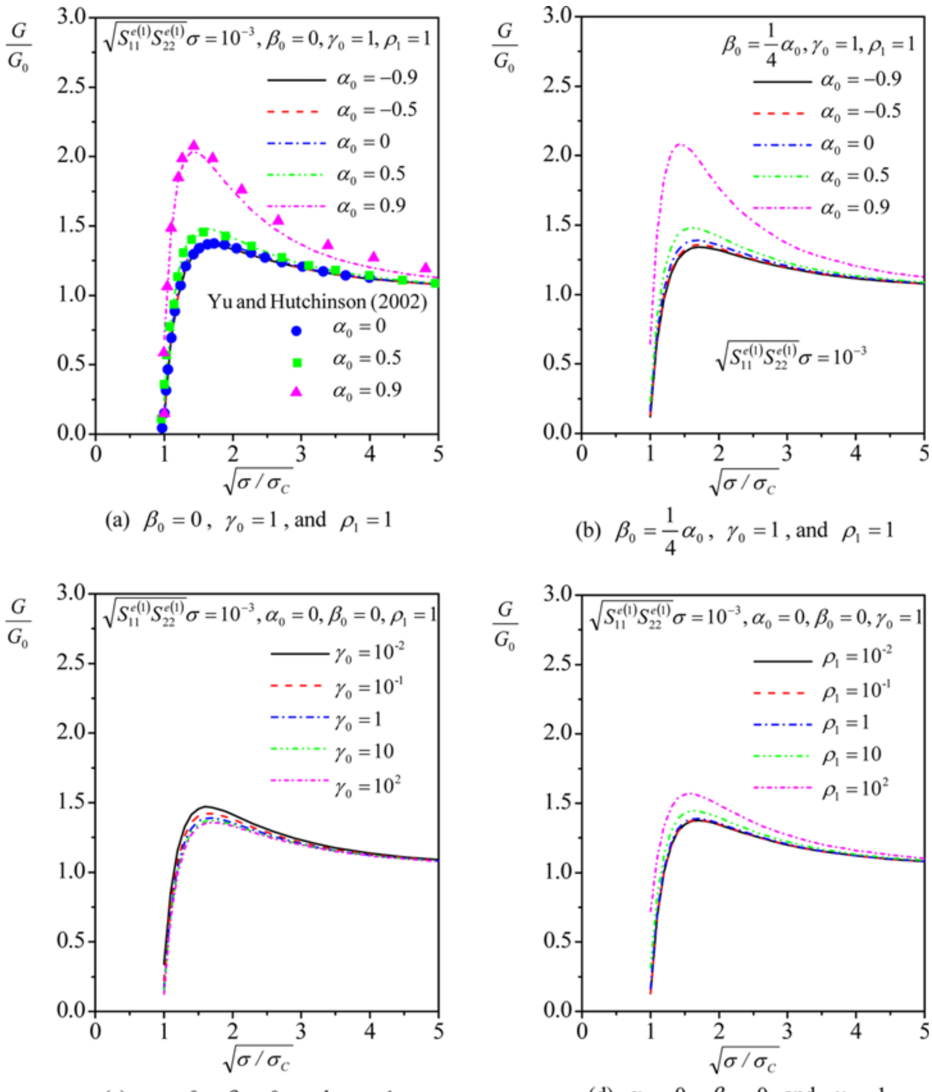

(a) $\beta_0=0$, $\gamma_0=1$, and $\rho_1=1$

(b) $\beta_0=\frac{1}{4}\alpha_0$, $\gamma_0=1$, and $\rho_1=1$

(c) $\alpha_0=0$, $\beta_0=0$, and $\rho_1=1$

(d) $\alpha_0=0$, $\beta_0=0$, and $\gamma_0=1$

Fig. 5 Normalized energy release rate G/G_0 as a function of $\sqrt{\sigma/\sigma_c}$ for $\sqrt{S_{11}^{e(1)}S_{22}^{e(1)}}\sigma=10^{-3}$

asymptotic value of 1. Fig. 5 shows that material parameters α_0, γ_0, and ρ_1 play an important role in determining G^* and that G^* is weakly dependent on β_0. In addition, G^* increases with an increase in α_0, which means that a more compliant substrate leads to a higher energy release rate. Moreover, an increase in γ_0 results in a decrease in G^*. In contrast to the case of γ_0, G^* increases with an increase in ρ_1. For high σ/σ_c values, the effect of all the material parameters on G^* is negligible.

The mode mixity of the interface crack is defined as

$$\psi=\tan^{-1}\frac{K_2^*}{K_1^*} \tag{41}$$

where ψ is the phase angle representing mode mixity and K_1^* and K_2^* are given by

$$\begin{Bmatrix} K_2^* \\ K_1^* \end{Bmatrix}=\mathbf{Y}(h^{i\varepsilon},h^{-i\varepsilon})\mathbf{k} \tag{42}$$

Here K_1^* and K_2^* have the same dimension as the classical stress intensity factor with the dimension of stress times the square root of the length. The matrix function $\mathbf{Y}$ is defined as

$$\mathbf{Y}(\zeta_1,\zeta_2)=\frac{1}{2}(\zeta_1+\zeta_2)\mathbf{I}+\frac{i}{2|\beta_0|}(\zeta_1-\zeta_2)\beta \tag{43}$$

where $\mathbf{I}$ is the identity matrix and β is the bimaterial matrix. Here β is

$$\beta=\begin{bmatrix} 0 & \beta_0 c \\ -\beta_0/c & 0 \end{bmatrix} \tag{44}$$

where

$$c=\lambda_1^{-\frac{1}{4}}\gamma_0^{-\frac{1}{4}}\sqrt{\frac{\left(1-\gamma_0^{\frac{3}{4}}\right)\alpha_0+\left(1+\gamma_0^{\frac{3}{4}}\right)}{\left(1-\gamma_0^{\frac{1}{4}}\right)\alpha_0+\left(1+\gamma_0^{\frac{1}{4}}\right)}} \tag{45}$$

The oscillatory index ε is

$$\varepsilon=\frac{1}{2\pi}\ln\frac{1+|\beta_0|}{1-|\beta_0|} \tag{46}$$

Here $\mathbf{k}$ is the interface stress intensity factor at the crack tip located at

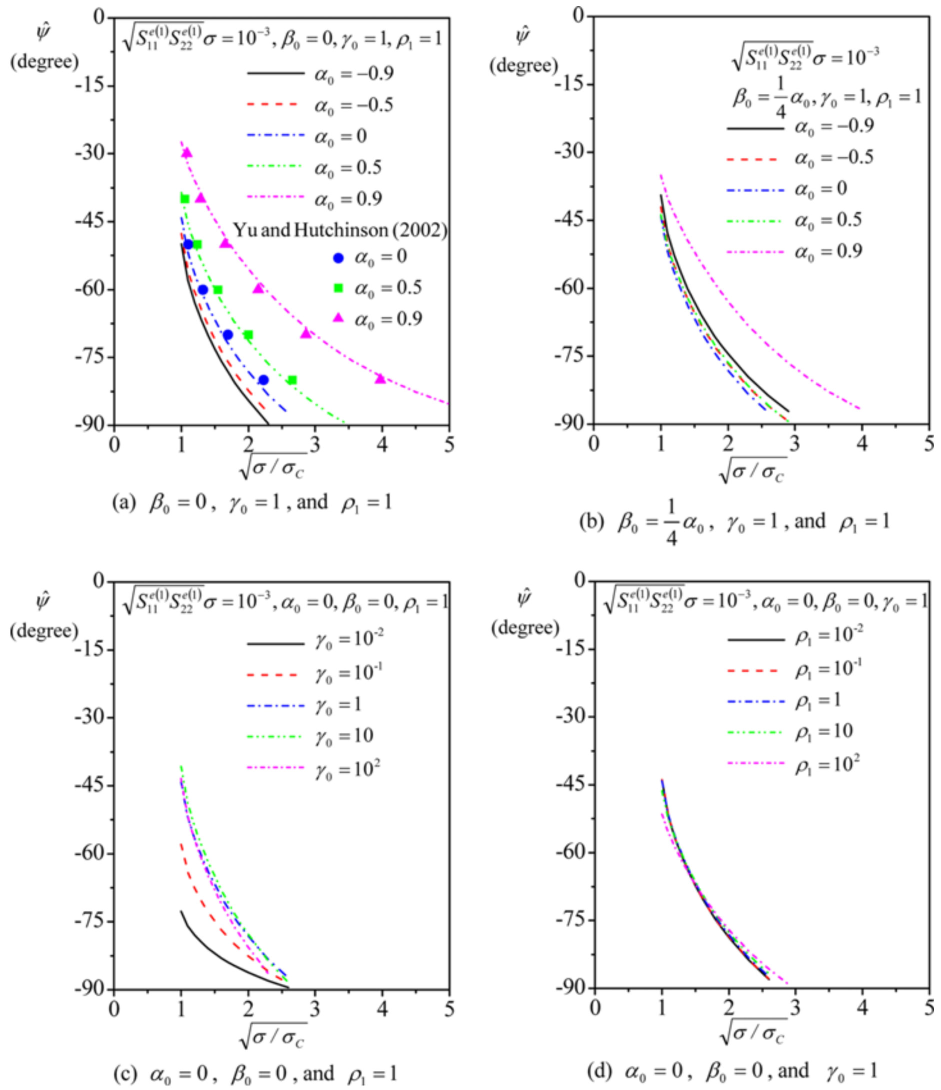

(a) $\beta_0=0$, $\gamma_0=1$, and $\rho_1=1$

(b) $\beta_0=\frac{1}{4}\alpha_0$, $\gamma_0=1$, and $\rho_1=1$

(c) $\alpha_0=0$, $\beta_0=0$, and $\rho_1=1$

(d) $\alpha_0=0$, $\beta_0=0$, and $\gamma_0=1$

Fig. 6 Mode mixity $\hat{\psi}$ as a function of $\sqrt{\sigma/\sigma_c}$ for $\sqrt{S_{11}^{e(1)}S_{22}^{e(1)}}\sigma=10^{-3}$

$x_1=b$ and $x_2=0$ and is defined as

$$\mathbf{k}=\begin{Bmatrix}K_2\\K_1\end{Bmatrix}=\lim_{x_1\to b^+}\sqrt{2\pi(x_1-b)}\,\mathbf{Y}((x_1-b)^{-i\varepsilon},(x_1-b)^{i\varepsilon})\begin{Bmatrix}\sigma_{21}(x_1,0)\\\sigma_{22}(x_1,0)\end{Bmatrix} \quad (47)$$

where σ_{ij} is stress. According to Beom et al.,[10] the mode mixity of the interface crack is given by

$$\tan\psi=\lambda_1^{-\frac{1}{4}}m\frac{h\Delta N\sin\omega+\sqrt{12}M_0\cos\omega}{h\Delta N\cos\omega-\sqrt{12}M_0\sin\omega} \quad (48)$$

Here

$$m=\sqrt{\frac{1-\alpha_{11}}{1-\alpha_{22}}} \quad (49)$$

$$\alpha_{11}=\frac{\left(1+\gamma_0^{\frac{1}{4}}\right)\alpha_0+\left(1-\gamma_0^{\frac{1}{4}}\right)}{\left(1-\gamma_0^{\frac{1}{4}}\right)\alpha_0+\left(1+\gamma_0^{\frac{1}{4}}\right)},\quad \alpha_{22}=\frac{\left(1+\gamma_0^{\frac{3}{4}}\right)\alpha_0+\left(1-\gamma_0^{\frac{3}{4}}\right)}{\left(1-\gamma_0^{\frac{3}{4}}\right)\alpha_0+\left(1+\gamma_0^{\frac{3}{4}}\right)} \quad (50)$$

In addition, ω has the following form:

$$\omega=\hat{\omega}(\alpha_0,\beta_0,\rho_1,\gamma_0)+\frac{1}{4}\varepsilon_0\ln\lambda_1 \quad (51)$$

where

$$\varepsilon_0=\frac{1}{2\pi}\ln\frac{1-\beta_0}{1+\beta_0} \quad (52)$$

The numerical results for $\hat{\omega}$ are given in Beom et al.[10] Substituting Eqs. (5) and (17) into Eq. (48) yields

$$\tan\psi=\lambda_1^{-\frac{1}{4}}m\frac{\left(\frac{\sigma}{\sigma_c}-\zeta\right)\tan\omega+\sqrt{12}\chi}{\left(\frac{\sigma}{\sigma_c}-\zeta\right)-\sqrt{12}\chi\tan\omega} \quad (53)$$

By introducing $\hat{\psi}$ defined as

$$\tan\hat{\psi}=m\frac{\left(\frac{\sigma}{\sigma_c}-\zeta\right)\tan\hat{\omega}+\sqrt{12}\chi}{\left(\frac{\sigma}{\sigma_c}-\zeta\right)-\sqrt{12}\chi\tan\hat{\omega}} \quad (54)$$

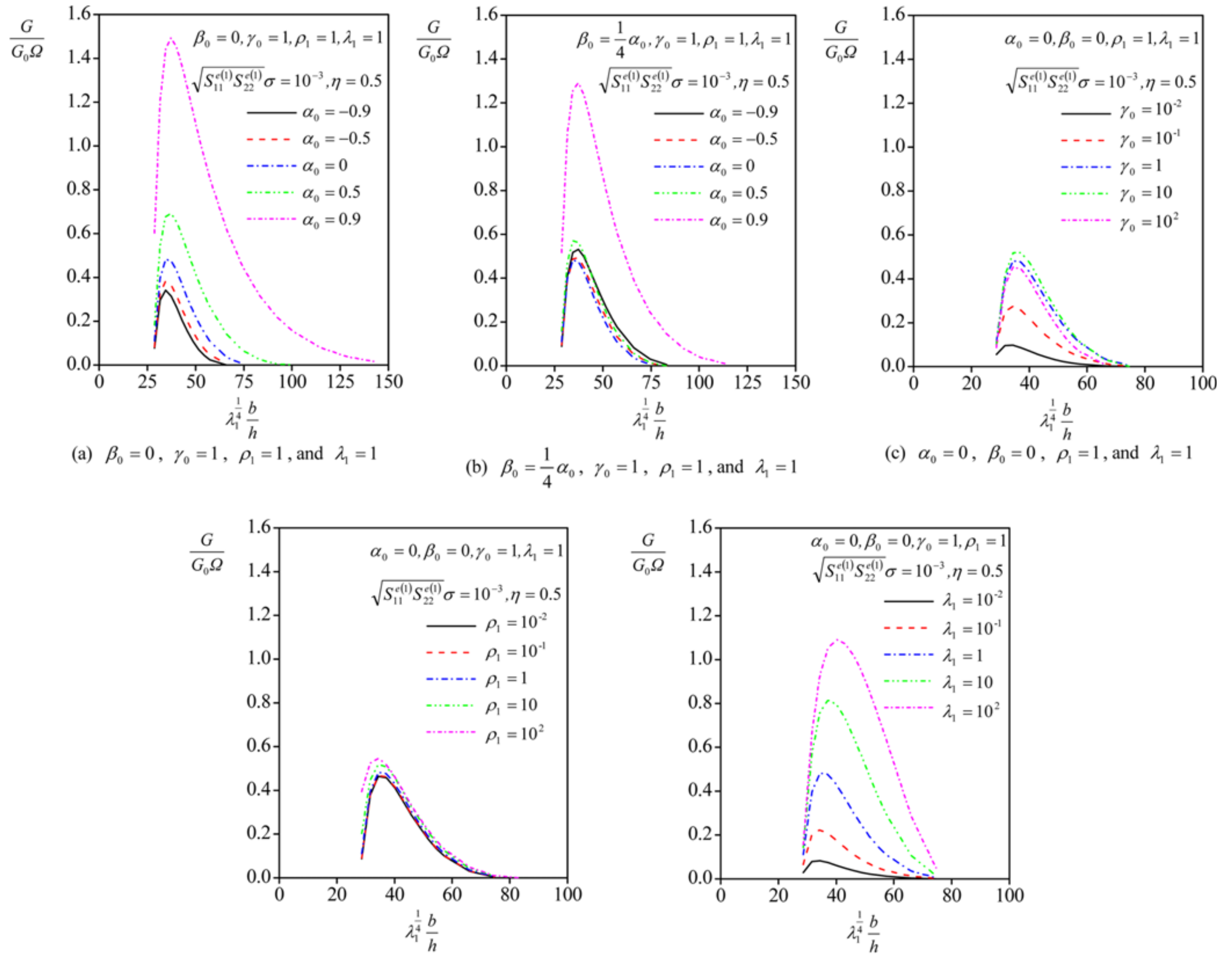

(a) $\beta_0=0$, $\gamma_0=1$, $\rho_1=1$, and $\lambda_1=1$

(b) $\beta_0=\frac{1}{4}\alpha_0$, $\gamma_0=1$, $\rho_1=1$, and $\lambda_1=1$

(c) $\alpha_0=0$, $\beta_0=0$, $\rho_1=1$, and $\lambda_1=1$

(d) $\alpha_0=0$, $\beta_0=0$, $\gamma_0=1$, and $\lambda_1=1$

(e) $\alpha_0=0$, $\beta_0=0$, $\gamma_0=1$, and $\rho_1=1$

Fig. 7 Normalized crack driving force $G/G_0\Omega$ as a function of $\lambda_1^{1/4}b/h$ for $\sqrt{S_{11}^{e(1)}S_{22}^{e(1)}}\sigma=10^{-3}$

Eq. (53) is recast as

$$\tan\psi = \lambda_1^{-\frac{1}{4}}\frac{\tan\hat{\psi}+m\tan\left(\frac{1}{4}\varepsilon_0\ln\lambda_1\right)}{1-\frac{1}{m}\tan\left(\frac{1}{4}\varepsilon_0\ln\lambda_1\right)\tan\hat{\psi}} \tag{55}$$

The phase angle function $\hat{\psi}$ depends only on six parameters ($\sqrt{\sigma/\sigma_c}$, $\sqrt{S_{11}^{e(1)}S_{22}^{e(1)}}\sigma$, α_0, β_0, γ_0, and ρ_1). Eq. (55) provides the explicit dependence of ψ on λ_1. If $\lambda_1=1$, then $\psi=\hat{\psi}$. For $\beta_0=0$, Eq. (55) gives

$$\tan\psi = \lambda_1^{-\frac{1}{4}}\tan\hat{\psi} \tag{56}$$

Mode mixity ψ decreases with an increase in λ_1 for $\beta_0=0$.

The phase angle function $\hat{\psi}$ is numerically calculated from Eq. (54). Here $\sqrt{S_{11}^{e(1)}S_{22}^{e(1)}}\sigma=10^{-3}$ is used. The numerical results for $\hat{\psi}$ are plotted as a function of $\sqrt{\sigma/\sigma_c}$ for various combinations of material parameters in Fig. 6. The numerical results for isotropic bimaterial cases are generally consistent with those in Yu and Hutchinson.[6] The magnitude of $\hat{\psi}$ increases with an increase in $\sqrt{\sigma/\sigma_c}$ and eventually reaches $\pi/2$, which is the pure mode II state for $\beta_0=0$. If $\beta_0=0$, $\gamma_0=1$, and $\rho_1=1$, then the bimaterial parameter α_0 has a significant effect on $\hat{\psi}$. The magnitude of $\hat{\psi}$ decreases as α_0 increases. For the case of $\beta_0=1/4\alpha_0$, $\gamma_0=1$, and $\rho_1=1$, the strong dependence of $\hat{\psi}$ on β_0 is observed, which stands in contrast to G^*. It is observed for $\alpha_0=0$ and $\beta_0=0$ from Fig. 6 that mode mixity $\hat{\psi}$ is strongly dependent on γ_0, whereas the effect of ρ_1 on $\hat{\psi}$ is negligible.

7. Discussion

The growth of the interface crack under mixed loading induced by buckling can be predicted based on the energy criterion. When the energy release rate G reaches the critical value

$$G = \Gamma(\psi) \tag{57}$$

where Γ is the fracture toughness of the interface crack that depends on mode mixity ψ, the crack advances along the interface. The interface toughness function is assumed to have the following form:[2]

$$\Gamma(\psi) = G_1^c\Omega(\psi) \tag{58}$$

$$\Omega(\psi) = 1 + (1-\eta)\tan^2\psi \quad (59)$$

where G_1^c is the toughness for $\psi = 0$ and η is the parameter adjusting the effect of the mode mixity. If the normalized crack driving force G^*/Ω satisfies

$$\frac{G^*}{\Omega(\psi)} < \frac{G_1^c}{G_0} \quad (60)$$

then there is no crack growth along the interface.

The crack driving force G^*/Ω depends on $\sqrt{S_{11}^{e(1)} S_{22}^{e(1)}}\sigma$, $\lambda_1^{1/4}b/h$, α_0, β_0, γ_0, ρ_1, and λ_1. Here close attention is paid to the effects of the material parameters on G^*/Ω Fig. 7 shows the numerical results for G^*/Ω as a function of $\lambda_1^{1/4}b/h$ for the given prestress $\sqrt{S_{11}^{e(1)} S_{22}^{e(1)}}\sigma = 10^{-3}$. In all computations, η=0.5 is chosen. In addition, G^*/Ω peaks and then decreases as $\lambda_1^{1/4}b/h$ increases regardless of the material parameter. This implies that the arrest of interface decohesion as a result of crack growth occurs, although the crack initially propagates from buckling. As shown in Fig. 7, the effects of all the material parameters (α_0, β_0, γ_0, ρ_1, and λ_1) on G^*/Ω are not negligible. With an increase in α_0, G^*/Ω increases, which indicates that a more compliant substrate results in a higher crack driving force. In other words, the interface crack induced by buckling is easier to extend along the interface if the substrate is more compliant. In addition, G^*/Ω increases with increases in γ_0, ρ_1 and λ_1, and β_0 has varying effects on the variation in G^*/Ω With a high degree of orthotropy, G^*/Ω is significantly different from that in the isotropic bimaterial case. Orthotropy parameters enhance or reduce the dimensionless crack driving force. Therefore, the solution for G^*/Ω in an isotropic bimaterial case has a limitation in predicting the growth of the interface crack in the orthotropic bimaterial structure for given prestress.

8. Concluding Remarks

This paper analyzed a buckled film bonded to an orthotropic substrate. The necessary material parameters for determining the energy release rate and mode mixity induced by film buckling were obtained by the analytical analysis. Numerical calculations were carried out to examine the effects of the material parameters on the energy release rate and mode mixity. Based on the numerical results for the energy release rate, the normalized crack driving force was evaluated and its dependence on material parameters was investigated. With a high degree of orthotropy, the normalized crack driving force is significantly different from that in the isotropic bimaterial case. Therefore, the application of the isotropic bimaterial solution to the prediction of crack growth in the orthotropic bimaterial structure is limited. The arrest of interface decohesion from crack growth occurs eventually and the critical width of the decohesion for crack arrest is dependent on material constants. The interface crack may be easier to propagate in a bimaterial with a more compliant substrate. These findings may shed some light on engineering design. A stiffer substrate may be used to reduce the possibility of growth of buckling delamination. A design of layered structures consisting of orthotropic materials based on analyses for isotropic materials may not be reliable.

ACKNOWLEDGEMENT

This research was supported by Basic Science Research Program through the National Research Foundation of Korea (NRF) funded by the Ministry of Education (NRF-2013R1A1A2A10008799).

REFERENCES

1. Whitcomb, J. D., “Parametric Analytical Study of Instability-Related Delamination Growth,” Composites Science and Technology, Vol. 25, No. 1, pp. 19-48, 1986.
2. Hutchinson, J. W. and Suo, Z., “Mixed Mode Cracking in Layered Materials,” Advances in Applied Mechanics, Vol. 29, pp. 63-191, 1991.
3. Choi, S. R., Hutchinson, J. W., and Evans, A. G., “Delamination of Multilayer Thermal Barrier Coatings,” Mechanics of Materials, Vol. 31, No. 7, pp. 431-447, 1999.
4. Bruno, D. and Greco, F., “An Asymptotic Analysis of Delamination Buckling and Growth in Layered Plates,” International Journal of Solids and Structures, Vol. 37, No. 43, pp. 6239-6276, 2000.
5. Cotterell, B. and Chen, Z., “Buckling and Cracking of Thin Films on Compliant Substrates under Compression,” International Journal of Fracture, Vol. 104, No. 2, pp. 169-179, 2000.
6. Yu, H. H. and Hutchinson, J. W., “Influence of Substrate Compliance on Buckling Delamination of Thin Films,” International Journal of Fracture, Vol. 113, No. 1, pp. 39-55, 2002.
7. Jeong, K. M. and Beom, H. G., “Buckling Analysis of an Orthotropic Layer Bonded to a Substrate with an Interface Crack,” Journal of Composite Materials, Vol. 37, No. 18, pp. 1613-1628, 2003.
8. Lu, T. Q., Zhang, W. X., and Wang, T., “The Surface Effect on The Strain Energy Release Rate of Buckling Delamination in Thin Film-Substrate Systems,” International Journal of Engineering Science, Vol. 49, No. 9, pp. 967-975, 2011.
9. Gurtin, M. E. and Murdoch, A. I., “A Continuum Theory of Elastic Material Surfaces,” Archive for Rational Mechanics and Analysis, Vol. 57, No. 4, pp. 291-323, 1975.
10. Beom, H. G., Cui, C. B., and Jang, H. S., “Dependence of Stress Intensity Factors on Elastic Constants for Cracks in an Orthotropic Bimaterial with a Thin Film,” International Journal of Solids and Structures, Vol. 49, No. 23, pp. 3461-3471, 2012.
11. Timoshenko, S. and Woinowsky-Krieger, S., “Theory of Plates and Shells,” McGraw-Hill New York, pp. 415-420, 1959.
12. Beom, H. G., Cui, C. B., and Jang, H. S., “Application of an Orthotropy Rescaling Method to Edge Cracks and Kinked Cracks in Orthotropic Two-Dimensional Solids,” International Journal of Engineering Science, Vol. 51, No. pp. 14-31, 2012.
13. Suo, Z. and Hutchinson, J. W., “Interface Crack between Two Elastic Layers,” International Journal of Fracture, Vol. 43, No. 1, pp. 1-18,

1990.

14. Beom, H. G. and Atluri, S. N., "Dependence of Stress on Elastic Constants in an Anisotropic Bimaterial under Plane Deformation and the Interfacial Crack," Computational Mechanics, Vol. 16, No. 2, pp. 106-113, 1995.

APPENDIX A. Derivation of Eq. (23)

A general solution for elastic fields for the problem of two-dimensional orthotropic plane strain can be written as follows:

$$\begin{Bmatrix} u_1 \\ u_2 \end{Bmatrix} = -2\mathrm{Re}[i\mathbf{H}\boldsymbol{\phi}(x_1,x_2)]\,,\quad \begin{Bmatrix} \sigma_{11} \\ \sigma_{12} \end{Bmatrix} = -2\mathrm{Re}\left[\frac{\partial}{\partial x_2}\boldsymbol{\phi}(x_1,x_2)\right],$$

$$\begin{Bmatrix} \sigma_{21} \\ \sigma_{22} \end{Bmatrix} = 2\mathrm{Re}\left[\frac{\partial}{\partial x_1}\boldsymbol{\phi}(x_1,x_2)\right],\quad \begin{Bmatrix} T_1 \\ T_2 \end{Bmatrix} = -2\mathrm{Re}[\boldsymbol{\phi}(x_1,x_2)] \tag{A.1}$$

where Re denotes the real part, T_i ($i = 1, 2$) is the resultant force,

$$\mathbf{H} = 2nS_{11}^e\begin{bmatrix} \lambda^{-\frac{1}{4}} & 0 \\ 0 & \lambda^{-\frac{3}{4}} \end{bmatrix} + i\begin{bmatrix} 0 & \sqrt{S_{11}^e S_{22}^e}+S_{12}^e \\ -(\sqrt{S_{11}^e S_{22}^e}+S_{12}^e) & 0 \end{bmatrix} \tag{A.2}$$

$$\phi_i(x_1,x_2) = \sum_{j,k=1}^{2} B_{ij}B_{jk}^{-1}g_k(z_j) \quad (i=1,2)$$

$$\mathbf{B} = \begin{bmatrix} -p_1 & -p_2 \\ 1 & 1 \end{bmatrix},\quad z_j = x_1+p_jx_2 \quad (j=1,2)$$

$$p_1 = \frac{i\lambda^{-\frac{1}{4}}}{\sqrt{2}}(\sqrt{\rho+1}+\sqrt{\rho-1})\,,\quad p_2 = \frac{i\lambda^{-\frac{1}{4}}}{\sqrt{2}}(\sqrt{\rho+1}-\sqrt{\rho-1}) \tag{A.3}$$

The function $g_i(z)$ ($i = 1, 2$) is a complex function of $z=x_1+px_2$, where p is a complex number with a positive imaginary part. Recently, Beom et al. [12] showed that the elastic representations in Eq. (A.1) hold for degenerate orthotropic materials with $p_1 = p_2$ as well as for orthotropic materials with $p_1 \neq p_2$.

The boundary conditions for the film/substrate structure in which the buckled part of the film is removed, as shown in Fig. 3(b), lead to

$$\begin{aligned}
&-2\mathrm{Re}\left[\sum_{j,k=1}^{2} B_{ij}^{(1)}p_j^{(1)}B_{jk}^{-1(1)}g'^{(1)}_k(x_1+p_j^{(1)}x_2)\right] = \begin{Bmatrix} \dfrac{\Delta N}{h}-\dfrac{12M_0}{h^3}\left(x_2-\dfrac{h}{2}\right) \\ 0 \end{Bmatrix} \\
&\qquad x_1 = \pm b,\quad 0<x_2\le h \\
&\mathrm{Re}[\mathbf{g}^{(2)}(x_1)] = \mathbf{0} \quad |x_1|<b \\
&\mathrm{Re}[\mathbf{g}^{(1)}(x_1)] = \mathrm{Re}[\mathbf{g}^{(2)}(x_1)] \quad |x_1|>b \\
&\mathrm{Im}[(\mathbf{I}-\boldsymbol{\alpha}-i\boldsymbol{\beta})\mathbf{g}^{(1)}(x_1)] = \mathrm{Im}[(\mathbf{I}+\boldsymbol{\alpha}+i\boldsymbol{\beta})\mathbf{g}^{(2)}(x_1)] \quad |x_1|>b \\
&\mathrm{Re}\left[\sum_{j,k=1}^{2} B_{ij}^{(1)}B_{jk}^{(1)-1}g'^{(1)}_k(x_1+p_j^{(1)}h)\right] = \mathbf{0} \quad |x_1|>b \quad x_2 = h \\
&\mathbf{g}^{(2)}(z) = \mathbf{0} \quad \sqrt{x_1^2+x_2^2}\to\infty \quad x_2<0
\end{aligned} \tag{A.4}$$

where ( )' indicates the derivative with respect to the associate argument and $\boldsymbol{\alpha}$ is the bimaterial matrix given as follows:[10,14]

$$\boldsymbol{\alpha} = \begin{bmatrix} \alpha_{11} & 0 \\ 0 & \alpha_{22} \end{bmatrix} \tag{A.5}$$

Given Eq. (A.4), the solution for $\mathbf{g}^{(j)}(z)$ ($j = 1, 2$) can be written in the following form:

$$\begin{aligned}
\mathbf{g}^{(j)}(z) = {}& \Delta N\mathbf{g}^{N(j)}\left(\frac{z}{h},\frac{b}{h},\alpha_0,\beta_0,\gamma_0,\rho_1,\lambda_1\right) \\
&+\frac{M_0}{h}\mathbf{g}^{M(j)}\left(\frac{z}{h},\frac{b}{h},\alpha_0,\beta_0,\gamma_0,\rho_1,\lambda_1\right)
\end{aligned} \tag{A.6}$$

where $\mathbf{g}^{N(j)}$ and $\mathbf{g}^{M(j)}$ ($j = 1, 2$) are dimensionless functions. With the condition of the resultant force for the symmetric problem

$$\mathbf{T}(-b,x_2) = \mathbf{T}(b,x_2) \quad 0<x_2\le h \tag{A.7}$$

it can be obtained from Eq. (A.1) that

$$\mathrm{Re}[\boldsymbol{\phi}(-b,x_2)-\boldsymbol{\phi}(b,x_2)] = \mathbf{0} \quad 0<x_2\le h \tag{A.8}$$

By using the relationship

$$u_1(-b,x_2) = -u_1(b,x_2) \quad 0<x_2\le h \tag{A.9}$$

in conjunction with Eqs. (A.1), (A.2), (A.6), and (A.8), the displacement $u_1(-b, x_2)$ can be written in the form of Eq. (22) with Eq. (23).

APPENDIX B. Derivation of Eq. (30)

To determine the dependence of compliance coefficients a_{ij} on the orthotropy parameter λ_1, the orthotropic rescaling technique developed by Beom et al.[10,12] is employed. Here the problem of plane strain is considered for the film/substrate structure mapped by the linear transformation:

$$\hat{x}_1 = x_1\,,\quad \hat{x}_2 = \lambda_1^{-\frac{1}{4}}x_2 \tag{B.1}$$

where the hat (^) indicates the quantity taken for the transformed problem. Therefore, the crack length and film thickness for the transformed problem are

$$\hat{b} = b\,,\quad \hat{h} = \lambda_1^{-\frac{1}{4}}h \tag{B.2}$$

Material constants for transformed solids are chosen as follows:

$$\begin{aligned}
&\hat{S}_{11}^{e(1)} = \lambda_1^{-\frac{1}{2}}S_{11}^{e(1)},\ \hat{S}_{22}^{e(1)} = \lambda_1^{\frac{1}{2}}S_{22}^{e(1)},\ \hat{S}_{12}^{e(1)} = S_{12}^{e(1)},\ \hat{S}_{66}^{e(1)} = S_{66}^{e(1)} \\
&\hat{S}_{11}^{e(2)} = \lambda_1^{-\frac{1}{2}}S_{11}^{e(2)},\ \hat{S}_{22}^{e(2)} = \lambda_1^{\frac{1}{2}}S_{22}^{e(2)},\ \hat{S}_{12}^{e(2)} = S_{12}^{e(2)},\ \hat{S}_{66}^{e(2)} = S_{66}^{e(2)}
\end{aligned} \tag{B.3}$$

The corresponding resultant force and bending moment for the transformed problem are, respectively,

$$\Delta\hat{N} = \lambda_1^{\frac{1}{4}}\Delta N\,,\quad \hat{M} = M \tag{B.4}$$

The displacement for the original problem can be obtained from the solution to the transformed problem as follows:[10,12]

$$u_1(x_1,x_2) = \hat{u}_1(\hat{x}_1,\hat{x}_2) \tag{B.5}$$

From Eqs. (22), (B.2), (B.4), and (B.5), it can be obtained that

$$u^N\left(\frac{x_2}{h}, \frac{b}{h}, \alpha_0, \beta_0, \lambda_1, \rho_1, \lambda_2\right) = \hat{u}^N\left(\frac{\hat{x}_2}{\hat{h}}, \frac{\hat{b}}{\hat{h}}, \hat{\alpha}_0, \hat{\beta}_0, \hat{\lambda}_1, \hat{\rho}_1, \hat{\lambda}_2\right),$$

$$u^M\left(\frac{x_2}{h}, \frac{b}{h}, \alpha_0, \beta_0, \lambda_1, \rho_1, \lambda_2\right) = \hat{u}^M\left(\frac{\hat{x}_2}{\hat{h}}, \frac{\hat{b}}{\hat{h}}, \hat{\alpha}_0, \hat{\beta}_0, \hat{\lambda}_1, \hat{\rho}_1, \hat{\lambda}_2\right) \quad \text{(B.6)}$$

By using Eqs. (28) and (B.6) in conjunction with

$$\hat{\alpha}_0 = \alpha_0\,,\ \ \hat{\beta}_0 = \beta_0\,,\ \ \hat{\gamma}_0 = \gamma_0\,,\ \ \hat{\rho}_1 = \rho_1\,,\ \ \hat{\lambda}_1 = 1 \qquad \text{(B.7)}$$

Eq. (30) can be derived.